

EuroSun 2012 – 6 Months Monitoring of Roof Integrated Modules and Performance Comparison in Different Installation Types

David Moser^{1*}, Walter Bresciani¹, Miglena Nikolaeva-Dimitrova¹, Laura Maturi¹

¹Institute for Renewable Energy, EURAC Research, Viale Druso 1, 39100 Bolzano (BZ), Italy

* Phone: +39 0471 055604; Fax: +39 0471 055699; E-mail: david.moser@eurac.edu

Abstract

The integration of PV modules in buildings is becoming day by day more important as in many countries policies are restricting the availability of large spaces for large PV plants installed on fixed racks. This delocalization of energy production on existing building surfaces (roofs and façades) present architectural and engineering challenges (e.g. Module/building material interface, working temperature etc.). In this work we present the results from 6 months monitoring of a 17.83 kWp system (three inverters) mounted three years ago on the roof of Milland Church in Bressanone (34° tilt angle, BZ, Italy). The performance ratio and final yield for the three strings are discussed together with the three parameter which mostly affect BIPV systems: temperature, shading and solar incident angle. The performance in a 6 months period (and following months) is presented and the results are compared with other installation types.

1. Introduction



Fig.1. PV roof installation at Milland Church in Bressanone, Italy

PV modules integrated in buildings not only produce electricity, but also replace normal building components and fulfil other functions required by the building envelope. This makes Building Integrated PV (BIPV) an interesting topic but also presents critical aspects like the reduction of PV efficiency due to the temperature of the panel, which increases if the back part is not aired, and the non-ideal angle of the installed modules. [1] Therefore, it becomes important to understand the behaviour of BIPV modules in operating conditions when they are installed next to other surfaces. A PV system installed on the roof of a building in Northern Italy has been analysed and monitored focusing on shading effects and comparison with other installation types. The PV system is integrated in the pitched roof of Milland Church in Bressanone (34° tilt angle, 203.5° azimuth angle, BZ, Italy) and it is in operation since August 2009 (see Fig 1). It is a retrofit system with 87 monocrystalline modules (17.83 KWp) with back-contact technology divided into three inverters (see Fig 2) (inverter 1 and 2 with 9 modules x 3 strings and inverter 3 with 11 modules x 3 strings).

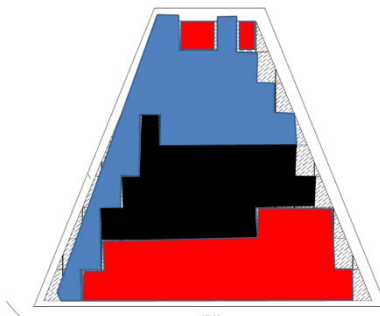


Fig.2. View of the roof from above: in blue are modules under inverter 1 (top), in black under inverter 2 (middle) and in red are modules under inverter 3 (bottom). The reference cell is positioned on the bottom edge of the roof, at the centre of the right half.

The shading diagram of the plant is shown in Fig 3. The monitoring system includes a meteorological station (1 minute interval averaged over 15 minutes) and a data logger for the registration of the PV system output (15 minutes interval). The former includes one humidity and temperature sensor, one c-Si reference cell (installed in August 2011) and two thermocouples (type K) which are positioned on the back side of two modules (under inverter 1 and 3). The PV output monitoring system collects data regarding the energy produced by the modules, DC and AC. The performance in a 6 months period (and following months) is presented and the results are compared with other installation types.

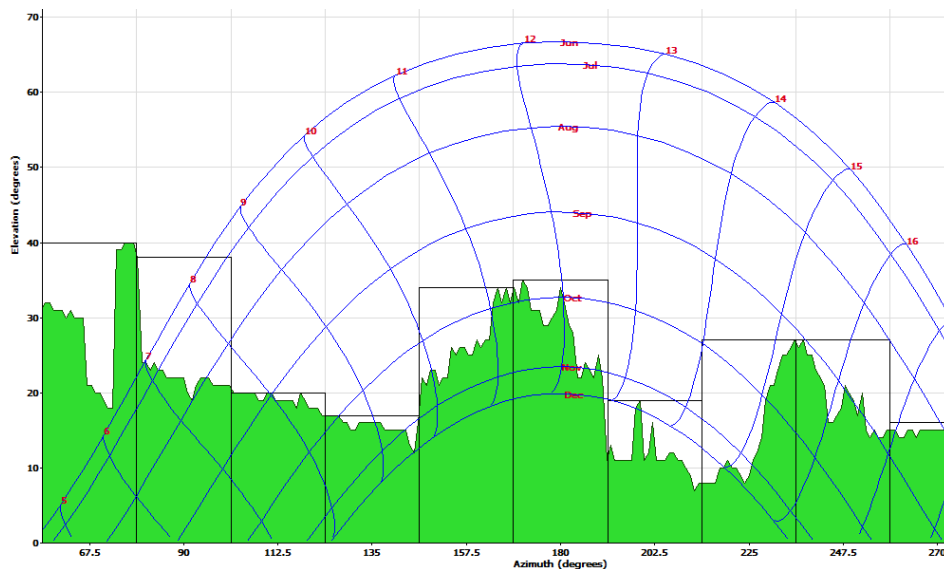


Fig. 3. Shading diagram taken in June 2012 from the reference cell. The shading in the range 140° - 190° and 225° - 240° are due to trees with maximum shading conditions (due to leaves and foliage). Shading changes seasonally.

2. Results and discussion

2.1. PR and Array Daily Yield

Fig. 4 shows the DC PR of the three inverters for the period August 2011-January 2012. Two main considerations can be derived from the graph: PR increases in winter for all three inverters with a higher increment for the strings under inverter 1 and 2 presenting values of PR above 1. These high values are due to an underestimation of the incoming radiation as it is measured close to the area

covered by modules under inverter 3 and is subject to shading from near objects in winter (Fig. 3). Energy losses due to shading are indeed quite high for inverter 3 as it is shown in Fig 5, where the average daily specific yield (DC values), Y_d , is plotted: this parameter corresponds to the equivalent number of hours in a day a plant would work at nominal power.

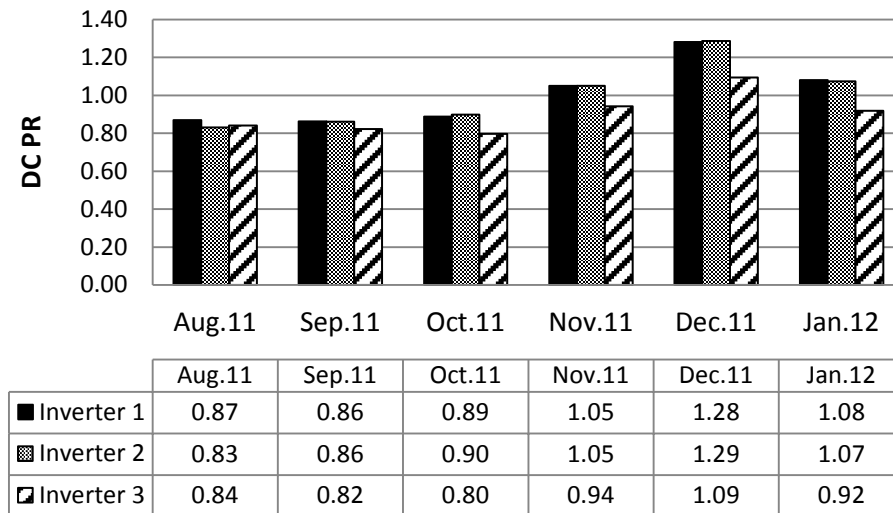


Fig. 4. DC Performance Ratio of strings under Inverter 1,2 and 3

From September onwards, modules under inverter 3 produce up to a 0.4 kWh/kW_p a day less than the other modules. The increase in PR towards winter is explained by better performance at lower working temperatures as expected for c-Si modules [2]. Nonetheless, the increment is a little too high than expected which might suggest that not all the area covered by inverter 3 is shaded with measured reference irradiance values which are not suitable for all modules.

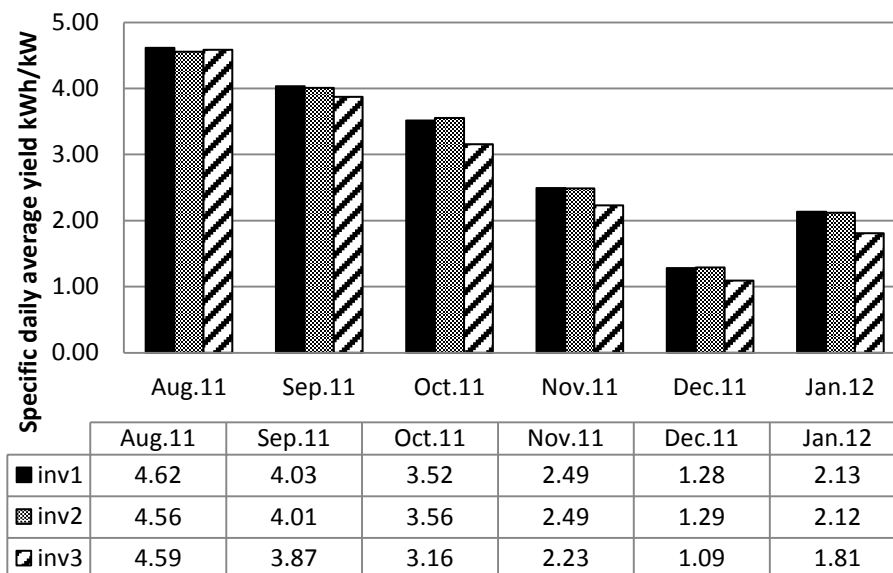


Fig. 5. Specific daily average yield of strings under Inverter 1,2 and 3

2.2. Filtering, PR_{STC} and temperature coefficients

Thus, shading and temperature losses need to be carefully considered. The performance ratio can be split into three components [3]

$$PR = PR_S \cdot PR_T \cdot PR_R \quad (1)$$

where PR_S is the shading loss factor, PR_T , the temperature loss factor, and PR_R the reflection loss factor due to the solar angle of incidence. The reflection loss factor does not affect the PR too much when the solar incident angle is perpendicular to the modules plane. PR_T is quite important due to the high temperature of the modules (up to 70°). The DC PR for modules under inverter 3 was calculated for each data point and plotted against the irradiance. Due to inhomogenous shading (clouds) and the position of the reference cell (close objects) the following scenarios can happen: a) reference cell is shaded while the modules are not or only partially, b) modules are partially shaded while the reference cell is not. As a consequence, the data in Fig 6 is very scattered and although the PR follows the expected trend against the irradiance, a second clustering of the data is present between $400\text{-}800\text{ W/m}^2$ with PR increasing with decreasing irradiance: this arises from an underestimation of the irradiance due to the aforementioned inhomogenous shading. From Fig 3, we can assume that PR_S is close to 1 during summer months with the plant affected by shading only in the early morning and late evening (no considerations can be made on PR_R). A temperature corrected PR value can then be calculated at this condition which is constant throughout the year.

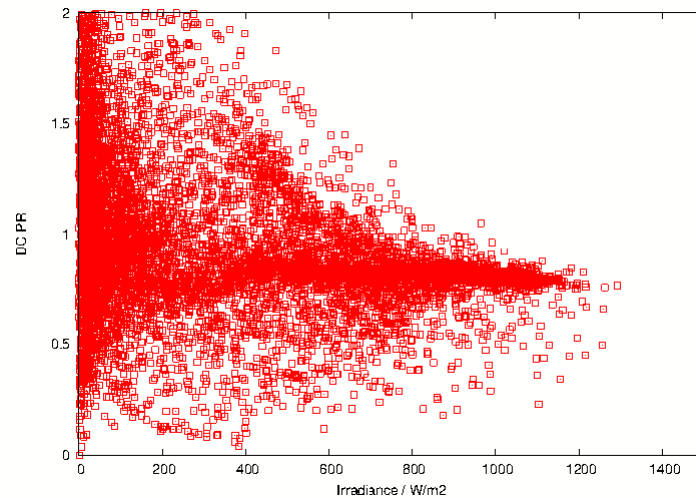


Fig. 6. DC PR (inverter 3) as a function of irradiance G

Fig 7 shows PR as a function of the module temperature at irradiance of 1000 W/m^2 (representative of summer months) where only values coming from days with daily yield Y_d higher than the average values calculated in Fig 5 are taken into account; this allows us to consider only data points from sunny days eliminating any other shading effects (clouds). From the PR definition, as P_{mpp} changes linearly with the temperature at constant irradiance, so does the PR. By fitting the data in Fig 7 with a linear equation it is then possible to extrapolate the PR_{STC} (spectral effects, e.g. $AM=1.5$, cannot be accounted for in this studies) at 25°C and 1000 W/m^2 obtaining a value of 0.852. From Fig 6, it is clear that, as expected, the values of PR are clustered around the range 0.6-1. This can be used as a filter to discriminate between homogenous and inhomogenous results when production is plotted as a function of irradiance and temperature.

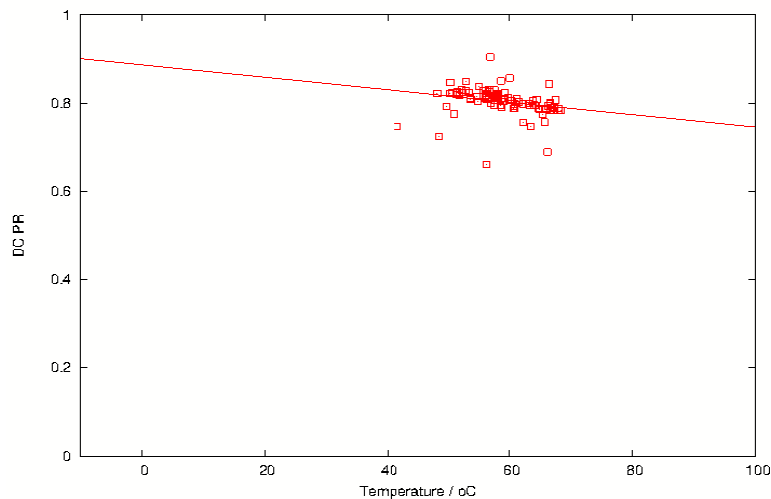


Fig. 7. Filtered ($Y_d > 5 \text{ kWh/m}^2$, $0.65 < PR < 0.95$) DC PR (inverter 3) at irradiance $G = 1000 \pm 20 \text{ W/m}^2$ as a function of temperature T_{mod}

Fig 8 shows all the data for DC power vs T_{mod} for three levels of irradiance, 1000 ± 10 , 700 ± 10 and $400 \pm 10 \text{ W/m}^2$. It is clear that a sorting procedure is needed (see Pichler et al [4]). Fig 9 shows the outcome of filtering by PR ($0.65 < PR < 0.95$); the data points are clustered and a linear behaviour of P_{mpp} vs T_{mod} is clearly visible with a resulting negative temperature coefficient ($\gamma_{25} = -11.18 \text{ W/}^\circ\text{C}$, $-0.18 \text{ \%/}^\circ\text{C}$ @ 1000 W/m^2 , $-9.22 \text{ W/}^\circ\text{C}$, $-0.21 \text{ \%/}^\circ\text{C}$ @ 700 W/m^2 , $-2.39 \text{ W/}^\circ\text{C}$, $-0.10 \text{ \%/}^\circ\text{C}$ @ 400 W/m^2). The trend for less negative temperature coefficients by decreasing irradiance in pc-Si modules was reported in the literature by King et al [5]. To be noted is that the filtering has a larger impact at low irradiance level while its impact is almost negligible at 1000 W/m^2 where in almost no occasion either the reference cell or the modules are shaded (reference cell is affected by shading from close object mainly around December where $G < 1000 \text{ W/m}^2$).

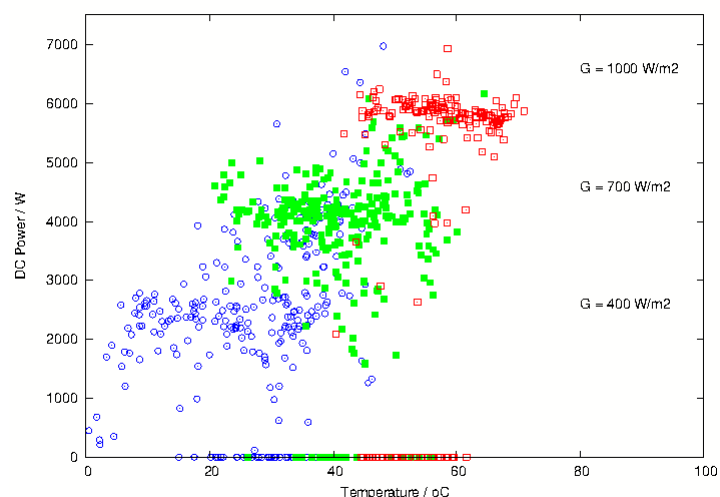


Fig. 8. DC Power as a function of module temperature at three irradiance level before filtering by PR

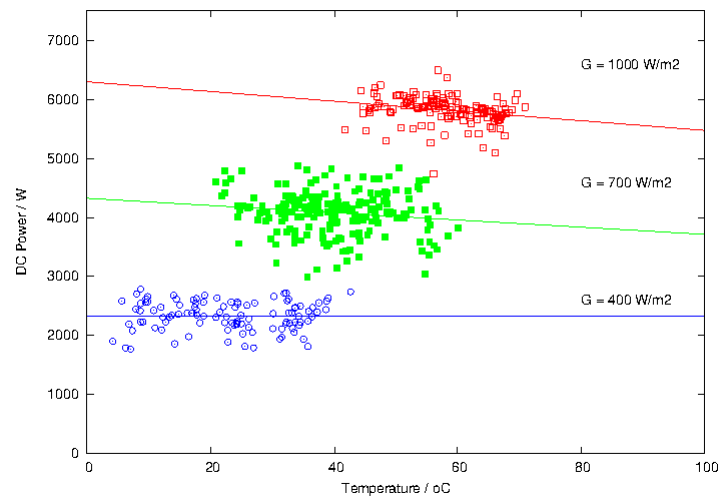


Fig. 9. DC Power as a function of module temperature at three irradiance level after filtering by PR

By knowing the temperature corrected value, it is possible to estimate the effect of modules shading due to near objects from September onwards. Shading of PV modules causes lower values of incoming irradiance with corresponding lower PR values, hence $PR_s > 1$ (see Fig. 6). The calculated DC PR values in Fig. 4 shows that in the period November-January, PR goes above 0.85 for inverter 3 (the temperature corrected PR value at 25°C, 1000 W/m²). This cannot just be explained by temperature effects as the module temperature at high irradiance levels (above 700 W/m²) is around 25°C. The high value of PR is then due, also for modules under inverter 3, to shading of the reference cell leading to inhomogenous data (reference cell is shaded more often than modules). This is particularly visible in December where PR is above 1 (1.09). However, a quantitative estimation of the losses in PR due to shading is made impossible by the inhomogeneity of the shading and the changing nature of the shading itself which is caused by near objects (trees with leaves and foliage).

2.3. Comparison of different installation types

The specific daily average yield shown in Fig. 5 can also be used to compare equivalent working hours at P_n with other installation types (all c-Si). Fig. 10 shows the comparison with a fixed rack installation (30° tilt angle, 172° azimuth angle) installed at the Airport Bolzano Dolomiti [6] and with a façade system installed in Bolzano city centre (90° tilt angle, 135° azimuth angle). The modules mounted on the roof (34° tilt angle) shows lower values for Y_d compared to a well ventilated fixed rack installation due to the higher operating temperature. Nevertheless, the yearly array yield for the 12 months period May 2011-April 2012 exceeds 1200 kWh/kW_p for all three inverters and specifically 1256 kWh/kW_p, 1243 kWh/kW_p, 1207 kWh/kW_p for inverter 1,2 and 3 respectively. This compares with $Y_a=1475$ kWh/kW_p for a pc-Si installed at ABD Airport on a fixed rack system (30° tilt angle) and $Y_a=761$ kWh/kW_p for the façade (90°). These values confirm the suitability of PV installations in the alpine region of Bolzano. On the façade system at this alpine latitude the equivalent working hours of the plant during summer months is halved compared to fixed rack. This difference is less during winter due to a higher incident angle of the sun.

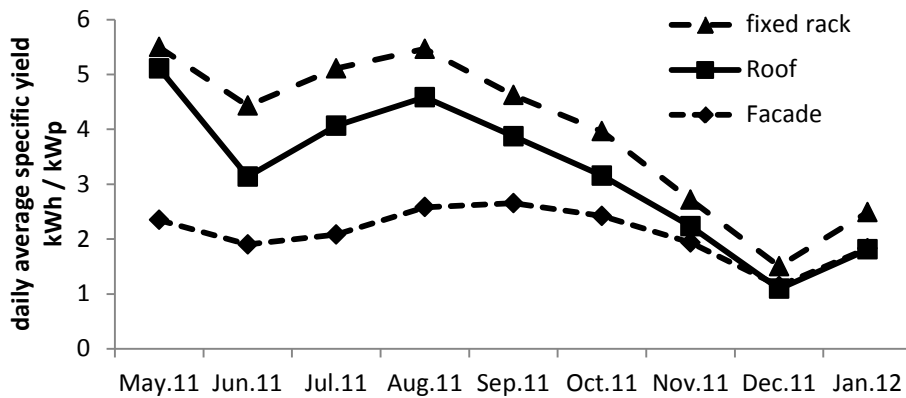


Fig. 10. Daily average specific yield for three different installations at similar latitude

In this study we have also investigated the availability in time of the produced energy using a monthly intermittency parameter (see Fig. 11) where 1 is zero production and 0 would correspond to 24 hours a day at nominal power.

$$IP = 1 - \frac{E}{24 \cdot d \cdot P_n} \quad (2)$$

where E is the energy produced, d is the number of days and P_n the nominal power. Such a parameter could be used to compare different renewable energy sources which all suffer from intermittency problems. In Fig 10 and 11, it is interesting to point out how the trend is similar for the three different installations with seasonal oscillations that peak in May (best scenario) and December (worst scenario).

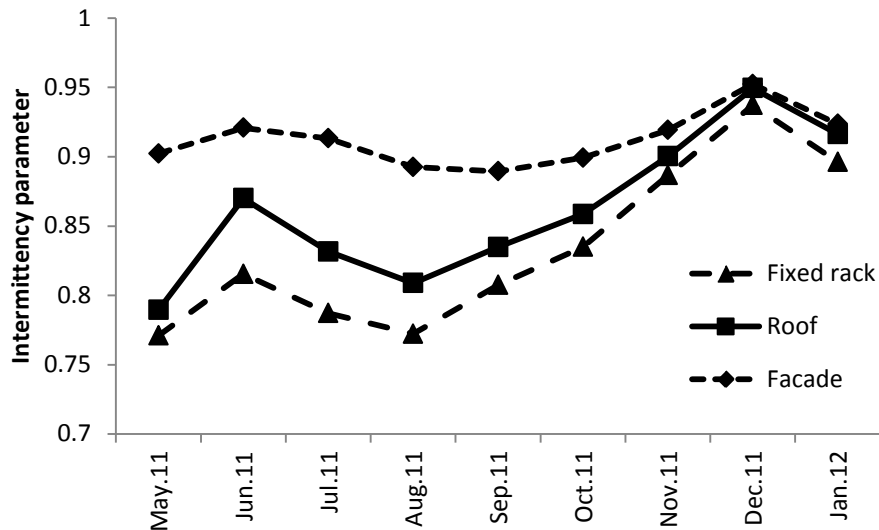


Fig. 11. Intermittency parameter for two different installations at similar latitude

3. Conclusions

The performance of a roof mounted PV system was reported with no significance losses in performance after 3 years of operation. The DC performance ratio of the plant shows some

problems (too high values, well above 1 during winter) due to inhomogeneous conditions in the modules-reference cell system. The reference cell is in fact shaded (but the modules are not or only partially) during winter due to the presence of near objects with the worst conditions found in December. In order to analyse homogenous data for the determination of temperature effects and correlation of irradiance G with the corresponding power P_{mpp} , a sorting procedure based on PR and daily average yield was implemented. This has a positive effective on the data and on the final outcome especially at low irradiance. The effects of shading from near objects were discussed with their influence on one of the three area of the plant (modules under inverter 3); a quantitative evaluation is made impossible by the changing nature of the shading conditions (trees as near objects). The temperature effect on P_{mpp} and consequently on PR was discussed where it was found that for the covered period (August 2011-January 2012), $PR_{STC} = 0.852$; spectral effects were not considered. It was found that the temperature coefficients are all negative at all irradiance levels but, as expected, they become less negative with decreasing irradiance. Daily average final yield and intermittency parameter were also compared with other installation types (fixed rack, facade) also based on c-Si module technology. The trend is similar for the three installations situated in the same geographic area; the roof installation presents a maximum in May with $5.1 \text{ kWh/kW}_p/\text{day}$ and $IP = 0.79$ and a minimum in December with $1.1 \text{ kWh/kW}_p/\text{day}$ and $IP = 0.95$. As expected, although the planning of the plant included solutions to improve ventilation, temperature effects are still predominant in the reduction of the performance during summer months while shading becomes more important during winter due to the higher incident angle.

References

- [1] L. Maturi, M. Armani, W. Bresciani, M. Del Buono, W. Sparber, “*PV roof integration, a case study in Northern Italy: how modules arrangement influences the PV performance*“, 24th PVSEC, 2009, 4256 – 4258
- [2] Wohlgemuth, J.H., Ransome, S.J., “*Performance of BP Solar Tandem Junction Amorphous Silicon Modules*” 2002. Twenty-Ninth IEEE Photovoltaic Specialists Conference, 2002, IEEE, pp. 1142– 1145
- [3] Soga K, Akasaka H, “*Influences of Solar Incident Angle on Power Generation Efficiency of PV Modules under Field Conditions*”, Journal of Asian Architecture and Building Engineering, **2**(2), 2003
- [4] Pichler M, “*Outdoor temperature coefficient of different PV module technologies at ABD-plant in a one-year period*”, MSc thesis, TUW-EURAC June 2012
- [5] David L King. “*Photovoltaic module and array performance characterization methods for all system operating conditions*” Aip Conference Proceedings, vol. **394**, no. 301, pages 347–368, 1997.
- [6] Colli A, Sparber W, Armani M, Kofler B, and Maturi L, “*Performance monitoring of different PV technologies at a PV field in northern Italy*”, 25th PVSEC, 2010, 4344 - 4349